

# TEMPERATURE DISTRIBUTIONS, THERMAL STRESSES AND THERMAL BUCKLING OF THIN SKINS SUPPORTED BY FRAMES

H. SCHUH

Senior Scientist, Thermodynamics, SAAB Aircraft Company, Sweden

## INTRODUCTION

In the analysis of structures in high-speed flight, a classical problem is to find the temperature distributions and thermal stresses in a skin-stiffener element (Fig. 1a); this structure was first treated by Hoff<sup>1</sup> and then by many other authors, see for instance.<sup>2,3,4</sup> In Fig. 1a the skin and the stiffener are assumed to be thin, so that in both the heat flow is one-dimensional. If the heat transfer is assumed to be uniform at the surface of the skin, then only the element within the lines *A-A* of the structure need be considered and this is replaced by the mathematical model of Fig. 1b. Although in the skin and the frame of Fig. 2 the section *A-A* could be derived from the element *A-A* of Fig. 1a by a thickening of the stiffener, the heat transfer conditions of the model of Fig. 1b cannot be made to correspond to those of Fig. 2, because the surface of the frame is exposed to external heat transfer. Hence the skin reinforced by a frame is a case not covered by solutions of Hoff's problem. Essentially, the present case differs from Hoff's case by the boundary condition for heat flow at the junction of the skin and the stiffener or frame. Because this boundary condition is more complicated in the present case, the analytical treatment of the heat flow in the structure is expected to become lengthy. Therefore a restricted case which appears to be of practical interest, is solved by analytical and by finite difference methods; of these the latter is in the present case simpler not only when using high-speed computers, but even when using only a desk calculating machine. The restricted case considered here is one in which the whole frame has a constant temperature. This is true if the depth of the frame is relatively small to moderate, or more precisely, if  $hl_2/k \ll 1$  ( $h$  = heat transfer coefficient,  $l_2$  depth of the frame,  $k$  = thermal conductivity).<sup>(5)</sup> With the help of finite difference methods more general cases can be solved, for instance those in which the external heat transfer depends in an arbitrary way on time and for which the standard analytical methods are not applicable.

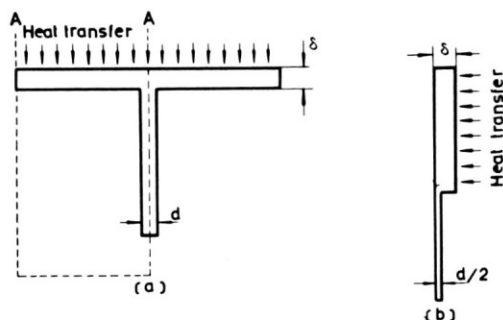


Fig. 1. Hoff's structure.

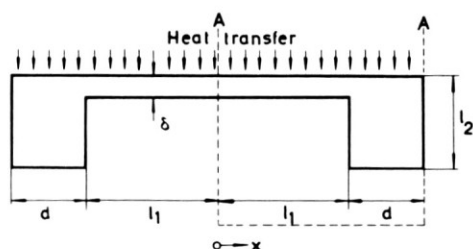


Fig. 2. Present structure.

### ANALYTICAL SOLUTION OF THE TEMPERATURE DISTRIBUTION IN THE RESTRICTED CASE

With uniform heat transfer along the surface of the skin and the frame, only part *A-A* of Fig. 2 need be considered. The heat flow is zero on all surfaces except those exposed to external heat transfer which is assumed to occur by a law, as that of forced convection. The equation for the heat flow in the skin with constant temperature across the thickness of the skin, reads:

$$\rho c \delta \frac{\partial T}{\partial t} = \delta k \frac{\partial^2 T}{\partial x^2} + h(T_f - T) \quad (1)$$

$\delta$  is the thickness of the skin,  $\rho$ ,  $c$ ,  $k$  are respectively the density, the specific heat and the heat conductivity of the material (all assumed constant),  $h$  the coefficient and  $T_f$  the reference temperature of the external heat transfer. A sudden start of motion with constant values of  $h$  and  $T_f$  is assumed in this section. Initially the temperature  $T_i$  is constant in the whole structure. Hence

$$t = 0, \quad T = T_i \quad (2)$$

Assume the same material in the skin and the frame; assume further, uniform temperature in the frame, then the boundary conditions (see also Fig. 2) are

$$x = 0; \quad \frac{\partial T}{\partial x} = 0 \quad (3)$$

$$x = l_1; \quad k\delta \frac{\partial T}{\partial x} + l_2 d\rho c \frac{\partial T}{\partial t} = -dh(T - T_f) \tag{4}$$

Introducing nondimensional quantities for the temperature, the distance along the skin, and the time, there is:

$$\Theta = (T - T_f)/(T_i - T_f); \quad \xi = x/l_1; \quad \tau = (kt)/(\rho cl_1^2) \tag{5}$$

further nondimensional parameters are:

$$R = \frac{l_2 d}{l_1 \delta}, \quad L = \frac{dh l_1}{\delta k}, \quad P = \frac{h l_1^2}{\delta k} \tag{6}$$

Introducing these quantities, one obtains for Eq. (1)

$$\frac{\partial \Theta}{\partial \tau} = \frac{\partial^2 \Theta}{\partial \xi^2} - P\Theta \tag{7}$$

the initial condition (2)

$$\tau = 0; \quad \Theta = 1 \tag{8}$$

and the boundary conditions (3) and (4)

$$\xi = 0, \quad \frac{\partial \Theta}{\partial \xi} = 0 \quad \text{and} \quad \xi = 1, \quad \frac{\sigma \Theta}{\partial \xi} + R \frac{\partial \Theta}{\partial \tau} = -L\Theta \tag{9}$$

Equation (7) can be simplified by a well-known transformation:<sup>6</sup>

$$\Theta = ue^{-P\tau} \tag{10}$$

Now the differential Eq. (7) becomes:

$$\frac{\partial u}{\partial \tau} = \frac{\partial^2 u}{\partial \xi^2} \tag{11}$$

the initial condition (8)

$$\tau = 0, \quad u = 1 \tag{12}$$

and the boundary conditions (9)

$$\xi = 0, \quad \frac{\partial u}{\partial \xi} = 0; \quad \xi = 1, \quad \frac{\partial u}{\partial \xi} + R \frac{\partial u}{\partial \tau} = -L^*u \tag{13}$$

where

$$L^* = L - PR \tag{14}$$

Next, a Laplace transformation is applied to Eqs. (11) and (13) observing Eq. (12). If  $\bar{u}$  is the transform of  $u$  and if  $p$  is the Laplace-transform variable, one obtains for Eq. (11)

$$\frac{d^2 \bar{u}}{d\xi^2} - p\bar{u} + 1 = 0 \quad (15)$$

and for Eq. (13):

$$\xi = 0, \quad \frac{d\bar{u}}{d\xi} = 0; \quad \xi = 1, \quad \frac{d\bar{u}}{d\xi} + R(p\bar{u} - 1) = -L^*\bar{u} \quad (16)$$

A solution of Eq. (15) with the boundary conditions [Eq. (16)] is:

$$\bar{u} = \frac{1}{p} - \frac{L^*}{p} \frac{\cosh \sqrt{p} \xi}{\sqrt{p} \sinh \sqrt{p} + Rp \cosh \sqrt{p} + L^* \cosh \sqrt{p}} \quad (17)$$

and using the inversion theorem the solution for  $u$  becomes:<sup>6</sup>

$$u = \frac{1}{2\pi i} \int_{\gamma-i\infty}^{\gamma+i\infty} \left[ \frac{1}{p} - \frac{L^*}{p} \frac{\cosh \sqrt{p} \xi}{\sqrt{p} \sinh \sqrt{p} + Rp \cosh \sqrt{p} + L^* \cosh \sqrt{p}} \right] e^{p\xi} dp \quad (18)$$

The integration is to be performed in the complex  $p$ -plane along a line from  $\gamma - i\infty$  to  $\gamma + i\infty$ , where  $\gamma$  is chosen so that all the singularities of the expression in the brackets [ ] in Eq. (18) lie to the left of that line. The integral is evaluated with the help of the calculus of residue.<sup>6</sup> The integrand becomes infinite at  $p = 0$  and at values of  $p$  satisfying

$$\sqrt{p} \sinh \sqrt{p} + Rp \cosh \sqrt{p} + L^* \cosh \sqrt{p} = 0 \quad (19)$$

This equation has no conjugate complex roots, as can be shown by methods given in Ref. 6. For real values of  $p = \lambda^2$  one obtains from Eq. (19):

$$\lambda \tanh \lambda = -R\lambda^2 - L^* \quad (20)$$

This equation has only one root  $\lambda = \lambda_0$  provided  $R$  and  $L^*$  have suitable values. For purely imaginary values of  $\sqrt{p} = i\lambda$ , one obtains from Eq. (19)

$$\lambda \tan \lambda = L^* - R\lambda^2 \quad (21)$$

The roots can be obtained in the usual way from the intersections of the curves  $z = \lambda \tanh \lambda$  and  $z = L^* - R\lambda^2$ .

There are an infinite number of discrete roots. The first term of the integrand in Eq. (18) yields 1 as a contribution to the integral. The residue at  $p = 0$  of

the second term yields  $-1$ ; with the contribution of the other residues one obtains finally:

$$u = \frac{2L^*e^{\lambda_0^2\tau} \cosh \lambda_0\xi}{[(L^* + R\lambda_0^2)^2 - \lambda_0^2(1 + R) + L^*] \cosh \lambda_0} + \sum_{n=1}^{\infty} \frac{2L^*e^{-\lambda_n^2\tau} \cos \lambda_n\xi}{[(L^* - R\lambda_n^2)^2 + \lambda_n^2(1 + R) + L^*] \cos \lambda_n} \tag{22}$$

where  $\lambda_0$  is the root of Eq. (20) and  $\lambda_n$  ( $n \geq 1$ ) are the roots of Eq. (21). With the help of Eq. (10) one obtains finally from Eq. (22):

$$\theta = \frac{2L^*e^{-(P-\lambda_0^2)\tau} \cosh \lambda_0\xi}{[(L^* + R\lambda_0^2)^2 - \lambda_0^2(1 + R) + L^*] \cosh \lambda_0} + \sum_{n=1}^{\infty} \frac{2L^*e^{-(\lambda_n^2+P)\tau} \cos \lambda_n\xi}{[L^* - R\lambda_n^2)^2 + \lambda_n^2(1 + R) + L^*] \cos \lambda_n} \tag{23}$$

Equation (23) gives the temperature distribution in the skin and the temperature of the frame follows also from Eq. (23) by putting there  $\xi = 1$ .

### THEMAL STRESSES AND THERMAL BUCKLING

Only elastic stresses are considered. It is further assumed that the cross sections of the heated structure remain plane and parallel to the position they had when the structure was at a uniform initial temperature  $T_i$ . No external forces are assumed to act on the structure. Hence thermal stresses  $\sigma$  are given by a well-known expression<sup>1-4</sup> which reads in the present case:

$$\sigma = E\beta(T_f - T_i) \left\{ \theta - \frac{\int_0^1 \theta d\xi + R(\theta)\xi_{-1}}{1 + R} \right\} \tag{24}$$

$E$  is the modulus of elasticity and  $\beta$  the coefficient of linear thermal expansion; both quantities are assumed constant. Compressive stresses are positive in Eq. (24). For determining critical values for buckling the (approximate) energy method<sup>7</sup> is used and the critical conditions for buckling are obtained from:

$$\delta_w(U_B + U_T) = 0 \tag{25}$$

where

$$\left\{ \begin{aligned} U_B &= \frac{D\psi}{2l_1^2} \int_0^1 \int_0^1 \left\{ \left( \frac{\partial^2 w}{\partial \xi^2} + \frac{1}{\psi^2} \frac{\partial^2 w}{\partial \eta^2} \right)^2 - \frac{2(1 - \nu_M)}{\psi^2} \left[ \frac{\partial^2 w}{\partial \xi^2} \frac{\partial^2 w}{\partial \eta^2} - \left( \frac{\partial^2 w}{\partial \xi \partial \eta} \right)^2 \right] \right\} d\xi d\eta \\ U_T &= -\frac{\delta}{2\psi} \int_0^1 \int_0^1 \sigma \left( \frac{\partial w}{\partial \eta} \right)^2 d\xi d\eta \end{aligned} \right. \tag{26}$$

and  $\delta_w$  indicates a differential variation with respect to one or more free parameters in  $w$ . In these equations (see also Fig. 3) there is:

$$D = \frac{E\delta^3}{12(1 - \nu_M^2)}, \quad \psi = \frac{l_0}{l_1}, \quad \xi = \frac{x}{l_1}, \quad \eta = \frac{y}{l_0} \quad (27)$$

further,  $\nu_M$  is Poisson's ratio,  $w$  is the deflection of the skin normal to its surface and  $l_1$  is the width of the skin. The extension of the structure in  $y$ -direction is unspecified, hence the variation of the deflection in  $y$ -direction is assumed such as to give minimum values of buckling. In view of what is known from exact solutions, one chooses for the deflection the expression

$$w = w_0(1 + \cos \pi\xi) \cos \frac{\pi}{2} \eta \quad (28)$$

This expression fulfills the boundary conditions for the skin being clamped at the frame (integral structure), hence at  $\xi = \pm 1$  there is  $w = 0$  and  $\partial w / \partial \xi = 0$ , and simply supported at  $\eta = \pm 1$  where  $w = 0$  (see Fig. 3). For convenience put

$$\sigma_{\text{crit}} = \frac{\pi^2 D}{4l_1^2 \delta} k_{\text{crit}} \quad (29)$$

If  $\sigma$  is constant, the min. critical value for buckling is known from an exact solution and it is  $k_{\text{crit}} = 6.99$  for  $\psi = 0.66$ . With this value for  $\psi$  and using the approximate expression [Eq. (28)] for  $w$ , one obtains  $k_{\text{crit}} = 7.26$  with the help of the energy method [Eqs. (25) and (26)]. This value for  $k_{\text{crit}}$  differs by 4% from the exact one. The energy method gives errors of about the same magnitude for nonuniform stress distributions corresponding to temperature distributions of a form encountered in problems similar to the present one.<sup>8</sup> Consider a sudden start of motion as above. The stresses are found by introducing the expression [Eq. (23)] for the temperature distribution in Eq. (24), and this yields:

$$\sigma = E\beta(T_f - T_i) \left\{ \Phi_0(\tau) \cosh \lambda_0 \xi + \sum_{n=1}^{\infty} \Phi_n(\tau) \cos \lambda_n \xi - K(\tau) \right\} \quad (30)$$

where

$$\left. \begin{aligned} \Phi_0(\tau) &= \frac{2L^* e^{-(P - \lambda_0^2)\tau}}{[(L^* + R\lambda_0^2)^2 - \lambda_0^2(1 + R) + L^*] \cosh \lambda_0} \\ \Phi_n(\tau) &= \frac{2L^* e^{-(P + \lambda_n^2)\tau}}{[(L^* - R\lambda_n^2)^2 + \lambda_n^2(1 + R) + L^*] \cos \lambda_n} \dots \\ & \qquad \qquad \qquad n = 1, 2, \dots, \end{aligned} \right\} \quad (31)$$

$$K(\tau) = \frac{1}{1 + R} \left[ \frac{\Phi_0(\tau) \sinh \lambda_0}{\lambda_0} + \sum_{n=1}^{\infty} \frac{\Phi_n(\tau) \sin \lambda_n}{\lambda_n} \right]$$

$$+ \frac{R}{1 + R} \left[ \Phi_0(\tau) \cosh \lambda_0 + \sum_{n=1}^{\infty} \Phi_n(\tau) \cos \lambda_n \right]$$

Next, the expression [Eq. (30)] for  $\sigma$  is introduced in Eq. (26); there  $U_T$  is proportional to an expression which is called a buckling parameter and is defined by:

$$\Delta_s = (T_f - T_i) \left[ \frac{3}{2} K(\tau) - \Phi_0(\tau) I_0 - \sum_{n=1}^{\infty} \Phi_n(\tau) I_n \right] \tag{32}$$

where

$$\left. \begin{aligned} I_0 &= \left[ \frac{3}{2\lambda_0} - \frac{2\lambda_0}{\lambda_0^2 + \pi^2} + \frac{\lambda_0}{2(\lambda_0^2 + 4\pi^2)} \right] \sinh \lambda_0 \\ I_n &= \frac{3}{2\lambda_n} \sin \lambda_n + \frac{\sin(\lambda_n - \pi)}{\lambda_n - \pi} + \frac{\sin(\lambda_n + \pi)}{\lambda_n + \pi} + \frac{\sin(\lambda_n - 2\pi)}{4(\lambda_n - 2\pi)} \\ &\quad + \frac{\sin(\lambda_n + 2\pi)}{4(\lambda_n + 2\pi)}, \dots, n = 1, 2, \dots \end{aligned} \right\} \tag{33}$$

Finally, the condition for buckling becomes, with the help of Eq. (25):

$$(\Delta_s)_{crit} = \Delta_M \equiv \frac{\delta^2}{(1 - \nu_M^2) l_1^2 \beta} \frac{\pi^2 \psi^2}{6} \left( 1 + \frac{1}{2\psi^2} + \frac{3}{16\psi^4} \right) \tag{34}$$

where  $\Delta_M$  is the critical parameter for buckling depending on the geometry and the properties of the structure, and the buckling pattern.

Equation (34) determines the time when buckling occurs.  $\psi = 0.66$  gives the minimum value of  $\Delta_M$  and hence in the present case the earliest possible buckling. It should be remembered that the expression for  $\Delta_s$  is valid for a sudden start of motion with constant flight conditions.

### THE INFLUENCE OF FLIGHT PARAMETERS

For aeronautical applications the solutions so far found are applicable only in particular cases. A sudden start of motion may be a good approximation to real conditions, for instance in the case of a change of flight speed of an aircraft in horizontal flight, but otherwise, particularly for missiles, this is not true. Before going into details heat transfer conditions are briefly discussed. Heat transfer is determined by two quantities  $h$  and  $T_f$  as follows from the equation:

$$q = h(T_f - T) \tag{35}$$

where  $q$  is the rate of local heat flow at the surface,  $h$  the heat transfer coefficient and  $T_f$  the friction temperature of adiabatic wall temperature (i.e., equal to the

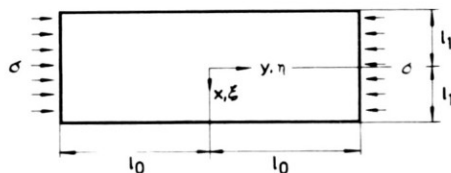


Fig. 3. Dimensions of and stresses acting on the skin.

wall temperature  $T$  in case  $q = 0$ ). The radiative heat transfer is neglected here as would be justified for flight at not-too-high altitudes ( $< 20$  km) and at not-too-high speeds ( $M \leq 5$  in the stratosphere). The heat transfer on the surface of the vehicle is determined by the development and the kind (laminar or turbulent) of the boundary layer in the external air flow.

The adiabatic wall temperature is for not-too-high speeds ( $M \leq 6$ ) approximately given by

$$T_f = T_1 \left( 1 + \frac{\gamma - 1}{2} \eta M^2 \right) \quad (36)$$

where  $\gamma = 1.40$  (air) is the ratio of the specific heats at constant pressure and at constant volume,  $\eta$  the recovery factor ( $= 0.90$  for turbulent and  $0.845$  for laminar boundary layers) and  $M = u/c_a$  the Mach number ( $u$  = the local velocity of the air flow,  $c_a$  the speed of sound) and  $T_1$  the static temperature, all values being taken locally at the outer edge of the boundary layer. Again for not-too-high speeds, local values may roughly be replaced by ambient values and  $u$  by the flight speed. Changes in altitude affect  $T_f$  only through changes in the ambient temperature which are moderate below the altitude of say,  $25$  km. However, the flight speed has a strong influence on  $T_f$ , for instance for  $M > 3$  there is roughly  $T_f \sim M^2$ .

The heat transfer coefficient may be approximated for the present purpose by flow conditions on an ideal flat plate at zero incidence. Thus for air ( $Pr = 0.71$ ) one obtains for not-too-high speeds:<sup>9</sup>

$$h = 0.61 \rho_a c_p u F \left( M, \frac{T}{T_1} \right) c_{fi} (Re_x) \quad (37)$$

where  $\rho_a$  and  $c_p$  are respectively the density and specific heat of the air at local conditions;\*  $T$  is the wall temperature,  $F(M, T/T_1) = c_f/c_{fi}$ ,  $c_f$  and  $c_{fi}$  the skin friction coefficient in compressible and incompressible flow respectively and  $Re_x = ux/v_a$  the Reynolds number with  $v_a = \mu/\rho_a$  as the kinematic viscosity,  $\mu$  as the dynamic viscosity of air (local values) and  $x$  the distance from the leading edge. In the following assume turbulent boundary layers which are most important for altitudes below  $25$  km. Then  $c_{fi}(Re_x)$  is roughly proportional to  $Re_x^{-1/6}$  and therefore  $h \sim \rho_a^{5/6}$ . Thus density has considerable influence on heat transfer and it in turn depends on the pressure which changes greatly with altitude; further  $\rho$  and  $F(M, T/T_1)$  depend on the static air temperature  $T_1$  which changes only moderately, as mentioned previously. The overall influence on  $h$  by  $u$  is moderate, because  $F(M, T/T_1)$  (see Ref. 9) and  $c_{fi}$  decrease with increasing  $u$ . In a typical application  $h$  changes about  $\pm 25$  percent from a mean value, if  $M$  varies between  $M = 2$  and  $4$ , the altitude being constant. For flight at constant altitude  $h$  may in many cases be assumed to be approximately constant, but this would not apply if considerable changes in altitude occurred.

\* At the outer edge of the boundary layer.



The standard analytical methods<sup>6</sup> for calculating transient temperatures allow for variations in  $T_f$ , but  $h$  must be constant.

According to Duhamels theorem one obtains:<sup>6</sup>

$$T - T_i = \int_0^\tau \Phi(\lambda) \frac{\partial}{\partial \tau} [1 - \Theta_s(\xi, \tau - \lambda)] d\lambda \tag{38}$$

where  $\Theta_s \dagger$  is the previous solution for a sudden start of motion,  $\lambda$  a variable of integration and  $\Phi(\tau) = T_f - T_i$ . This method can be applied to any linear combination of the temperatures and their spatial mean values, hence also to the buckling parameter  $\Delta$ :

$$\Delta = \int_0^\tau \Phi(\lambda) \frac{\partial}{\partial \tau} [\Delta_s(\tau - \lambda)] d\lambda \tag{39}$$

where  $\Delta_s(\tau)$  is the buckling parameter for a sudden start of motion as given by Eq. (32);  $\Delta_s$  is zero at  $\tau = 0$ . If  $\Phi(\tau)$  is an arbitrary function of time, the calculation of  $\Delta$  with the help of Eq. (39) becomes in general tedious and is more conveniently replaced by an approximate method to be discussed later on.

First, consider the particular case

$$\Phi = B\tau \tag{40}$$

which allows the integral in Eq. (39) to be evaluated exactly. With  $\Delta_s$  from Eq. (32) the solution is

$$\Delta \ddagger(\tau) = B \left\{ A_0 \ddagger \left( 1 - e^{-(P - \lambda_0^2)\tau} \right) + \sum_{n=1}^\infty A_n \ddagger \left( 1 - e^{-(P + \lambda_n^2)\tau} \right) \right\} \tag{41}$$

with

$$\left. \begin{aligned} A_0 \ddagger &= \frac{\Phi_0(0)}{P - \lambda_0^2} \left[ \frac{3}{4} \left( \frac{\sinh \lambda_0}{\lambda_0} + \cosh \lambda_0 \right) - I_0 \right] \\ A_n \ddagger &= \frac{\Phi_n(0)}{P + \lambda_n^2} \left[ \frac{3}{4} \left( \frac{\sin \lambda_n}{\lambda_n} + \cos \lambda_n \right) - I_n \right] \end{aligned} \right\} \tag{42}$$

If  $\Phi$  is an arbitrary function of  $\tau$ , replace  $\Phi$  in the  $(\Phi - \tau)$  diagram by a sequence of straight lines as shown in Fig. 4. At the times  $\tau_1, \tau_2, \dots$ , changes

†  $1 - \Theta_s$  is zero at  $\tau = 0$ , as required by Duhamels' theorem in the form presented in Ref. 6.

‡ 1 kp = 1 kg weight = 2.205 lb.

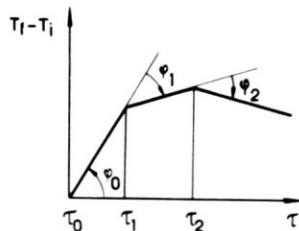


Fig. 4. A variation of  $T_f - T_i$  in form of a sequence of straight lines.

in direction occur by amounts  $\varphi_1, \varphi_2, \dots$ , ( $\varphi$  positive when anticlockwise). Using the principle of superposition the solution for  $\tau_{N-1} \leq \tau \leq \tau_N$  is

$$\Delta = \sum_{n=0}^{N-1} B_n \Delta \ddagger (\tau - \tau_n), \quad B_n = S \tan \varphi_n \quad (43)$$

where  $S$  is a suitable scale factor. With this procedure the possibilities of standard analytical methods seem to be exhausted. It is useful to consider now examples.

### EXAMPLES

Consider a light alloy structure with the following thermal properties:  $\rho c = 609$  kcal/m<sup>3</sup>°C,  $k = 0.03$  kcal m sec°/C,  $\beta = 23 \times 10^{-6}$ /°C and the mechanical properties  $E = 7.2 \times 10^3$  kp/mm<sup>2</sup>‡,  $1 - \nu_M^2 = 0.9$ .

Assume all material properties to be constant up to a temperature of 250°C and assume Hook's law to be valid up to about  $\sigma_p = 20$  kp/mm<sup>2</sup>. Certain types of available aluminum alloys correspond approximately to these assumptions, but these alloys need not necessarily be good materials for structures at elevated temperatures from an overall engineering point of view. The dimensions of the structure are:  $\delta = 2$  mm,  $d = 10$  mm,  $l_1 = 75$  mm and  $l_2 = 15$  mm. Throughout this chapter a constant heat transfer coefficient of  $h = 0.07$  kcal/m<sup>2</sup>/sec°/C is assumed. This value is representative for flight between  $M = 2$  and 4 at 11 km altitude with turbulent boundary layers at the surface of the vehicle. In seeking solutions by analytical methods the eigenvalues  $\lambda_0, \lambda_1, \dots$ , are found from Eqs. (20) and (21) and numerical values for the present example are given in Table 1. For the present example the critical parameter for buckling is  $\Delta_M = 77.1$ °C from Eq. (34). For a sudden start of motion and  $T_f - T_i = 250$ °C (corresponding, for instance, roughly to an increase in Mach number from  $M = 0.9$  to  $M = 2.7$  at 11 km altitude and turbulent boundary layer flow)  $\Delta_M$  is reached at 18.3 sec, according to Eq. (32).§ The critical temperature and stress distributions according to Eqs. (23) and (24) respectively are given in Fig. 5. The maximum stress at  $\xi = 0$  is equal to 9.1 kp/mm<sup>2</sup> and lies below the assumed limit for elastic behavior.

Next assume linearly increasing  $T_f - T_i$ , i.e.,  $\Phi = T_f - T_i = B\tau$ . Assuming  $B = 3120$ °C (equal to an increase of 27.4°/sec), buckling would occur at  $t = 15$  sec and corresponding temperature and stress distributions are given in Fig. 6.

TABLE I

$\lambda_0$	$\lambda_1$	$\lambda_2$	$\lambda_3$	$\lambda_4$	$\lambda_5$
1.9599	1.7680	4.8762	7.9686	11.0816	14.2055

‡ 1 kp = 1 kg weight = 2.205 lb.

§ Here and in the following examples an initial temperature of +30°C was assumed.

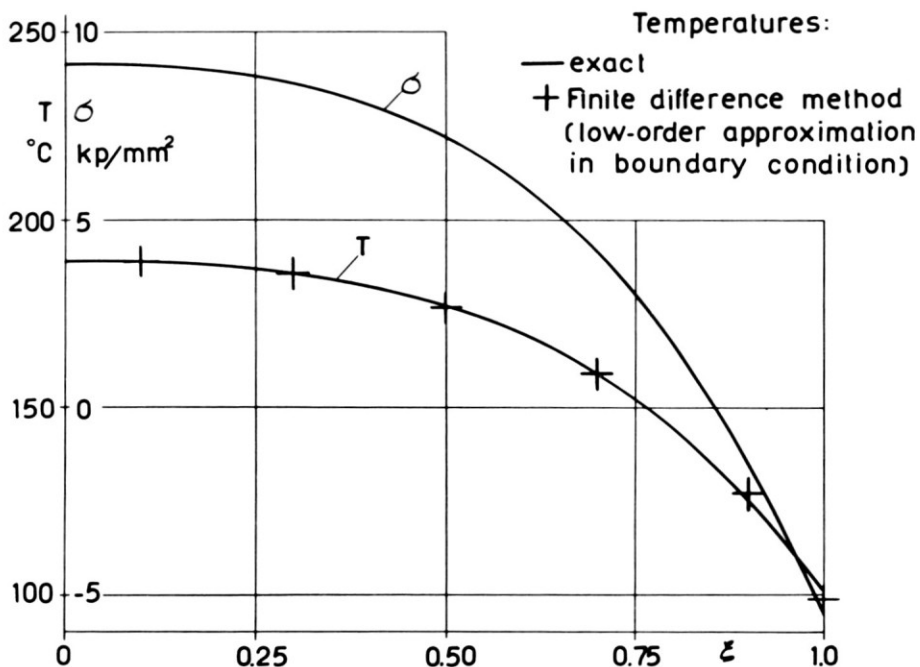


Fig. 5. Case of sudden start of motion.

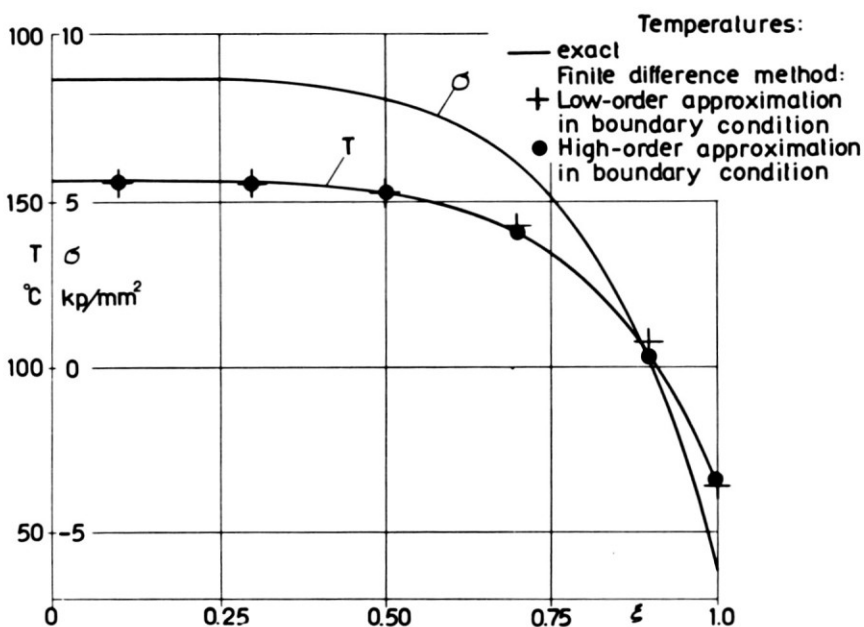


Fig. 6. Case of linear increase in speed.

As a third example, consider a motion leading to a sequence of two straight lines in the  $\Phi - \tau$  diagram as in Fig. 7; this may roughly correspond to the flight of a rocket-propelled missile. Assume for  $\Phi$  a linear increase of  $500^\circ\text{C}$  within 4 sec, followed by a decrease in  $\Phi$  of  $25^\circ\text{C}/\text{sec}$ . The buckling parameter  $\Delta$  is calculated with the help of Eq. (43) and buckling occurs at  $t = 7.45$  sec; the critical temperature and stress distributions are given in Fig. 8.

The critical temperature and stress distributions are rather similar in all three cases. Due to the more rapid heating in the third case, the temperature in the skin is uniform over a somewhat wider region than in the other cases. In all cases the critical stress in the middle of the skin ( $\xi = 0$ ) is slightly above the corresponding value for the isothermal case ( $\sigma_{\text{crit}} = \text{const.} = 8.5 \text{ kp}/\text{mm}^2$ ). The explanation is that the skin is clamped at the frame and therefore the stresses in the middle of the skin are mainly responsible for buckling.

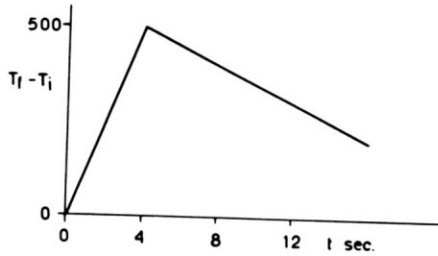


Fig. 7. Variation of friction temperature  $T_f$  with time (rocket-propelled missile).

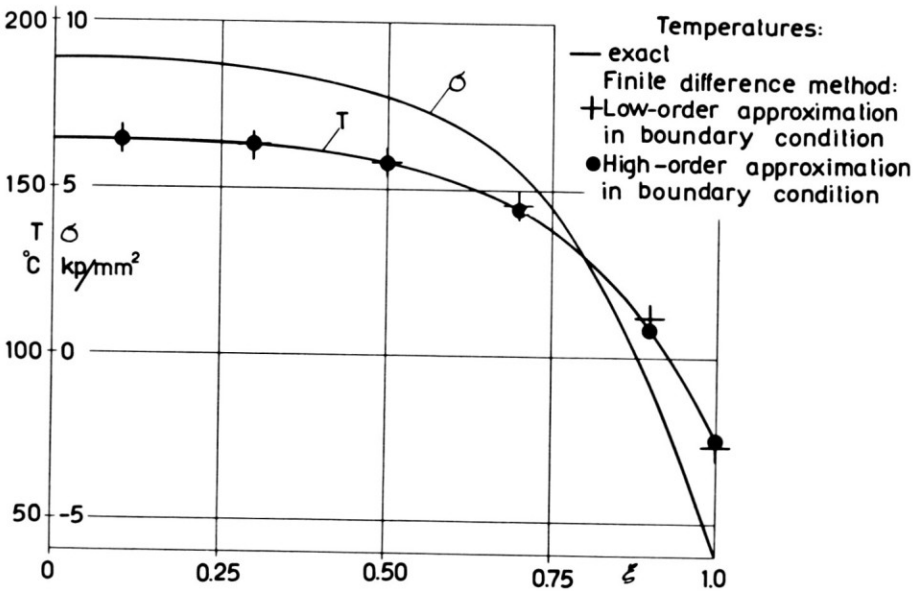


Fig. 8. Case of rocket propelled missile with  $T_f$  as in Fig. 7, but heat-transfer coefficient assumed constant.

## CALCULATION OF TEMPERATURE DISTRIBUTIONS BY FINITE DIFFERENCE METHODS

It is recalled that standard analytical methods for calculating heat flow in solids are limited to convection-type heat transfer with constant values of  $h$ ; further, it appears to be cumbersome to extend these methods from the restricted cases, so far treated, to general cases with nonuniform temperatures in the frame.

However, finite difference methods, although approximate in a strictly mathematical sense, are free from the above limitations; besides they are more suitable for high-speed computers than analytical methods. Finite difference methods were introduced about forty years ago, but it is only in the last 15 years that they have received much attention and now at least two books deal with them from a rigorous mathematical point of view.<sup>10,11</sup> There the behavior of finite difference solutions is investigated in the limiting case of vanishing differences of the independent variables of space and time; these are  $\Delta x$  and  $\Delta t$  respectively in case of one-dimensional heat flow. However, the computational work increases greatly with decreasing size of  $\Delta x$  and  $\Delta t$ , while in the case of applications the required accuracy of the solutions is always limited because of uncertainties in the knowledge of the material properties and of the external heat transfer. Hence the behavior of finite difference solutions for any finite size of  $\Delta x$  and  $\Delta t$  would be of more interest for applications. A beginning of such investigations has been made<sup>5,12</sup> and some of these results are applied to the present problem.

Here a finite difference method of the explicit type is used and the procedures of Refs. 5, 12 are followed. Replace in Eq. (1) the expressions  $\partial T/\partial t$ ,  $\partial^2 T/\partial x^2$  and  $T - T_f$  by  $(T_{n, m+1} - T_{n, m})/\Delta t$ ,  $(T_{n+1, m} + T_{n-1, m} - 2T_{n, m})/(\Delta x)^2$  and  $(1/2)\{[h(T_f - T)]_m + [h(T_f - T)]_{m+1}\}$  respectively, where  $T_{n, m}$  is the temperature at  $x = m\Delta x$  and  $t = n\Delta t$ . Then the finite difference equations for calculating the temperature of the skin becomes

$$T_{n, m+1} = \frac{1}{1 + p_h} [p(T_{n-1, m} + T_{n+1, m}) + (1 - 2p - p_h)T_{n, m} + p_h(T_{f, m} + T_{f, m+1})] \quad (44)$$

where

$$p = \frac{\kappa \Delta t}{(\Delta x)^2} \quad \text{and} \quad p_h = \frac{h \Delta t}{2\rho c \delta} \quad (44a)$$

( $\kappa = k/\rho c =$  thermal diffusivity). The truncation error of Eq. (44), defined as  $E_{n, m} = (T_{n, m+1})_{\text{exact}} - (T_{n, m+1})_{\text{diff. method}}$  is of the order of magnitude

$$O \left[ (\Delta x)^4 \frac{\partial^4 T}{\partial x^4} \right] + O \left[ (\Delta x)^4 \frac{\partial^4 T}{\partial x^2 \partial t} \right]$$

using the relation  $\Delta t \leq (a/\kappa)(\Delta x)^2$  which follows from the stability condition for Eq. (44) and where  $a \leq 1/[2 + h(\Delta x)^2/(2\delta k)]$  (Ref. 12). Auxiliary points 0

and  $N + 1$  (see Fig. 9) are used for satisfying boundary conditions,<sup>12</sup> so that the boundaries lie midway between the pairs of points 0, 1 and  $N, N + 1$  (see Fig. 9). Then Eq. (3) becomes

$$T_{0, m} = T_{1, m} \tag{45}$$

Put for  $(\partial T/\partial t)_{l_i} = (\frac{1}{2} \Delta t)(T_{N+1, m+1} + T_{N, m+1} - T_{N+1, m} - T_{N, m})$  and  $(T)_{l_i} = (\frac{1}{4})(T_{N+1, m+1} + T_{N+1, m} + T_{N, m+1} + T_{N, m})$ . In the latter expression the temperature is also a mean between the times  $t = m\Delta t$  and  $t = (m + 1)\Delta t$  according to Ref. 12. With  $(\partial T/\partial x)_{l_i} = (1/\Delta x)(T_{N+1, m} - T_{N, m})$ // the finite difference equivalent to Eq. (4) becomes finally

$$T_{n+1, m+1} = \frac{1}{1 + p_f} \{ (1 - p_f - p_r)T_{N+1, m} + (1 - p_f + p_r)T_{N, m} - (1 + p_f)T_{N, m+1} + 2p_f(T_{f, m} + T_{f, m+1}) \} \tag{46}$$

where

$$p_r = \frac{2\Delta\tau}{R\Delta\xi} \quad \text{and} \quad p_f = \frac{L\Delta\tau}{2R} \tag{47}$$

for  $L$  and  $R$  see Eq. (6);  $\Delta\tau = (k\Delta t)/\rho c l_1^2$  and  $\Delta\xi = \Delta x/l_1$  according to Eq. (5). Because of symmetry the first boundary condition [Eq. (45)] has no truncation error; for the second, Eq. (46), it is

$$O \left[ (\Delta x)^2 \left( \frac{\partial^2 T}{\partial x^2} \right)_{N+1/2, m+1/2} \right]$$

This truncation error is of a higher order of magnitude than that for interior points (see above). The skin in the example of section 5 is divided into  $N = 5$  sections; then according to Ref. 12 the error in the temperatures of the skin would at most be about 1% of  $T_f - T_i$ . As a time step  $\Delta t = 1$  sec was chosen, a value somewhat below the highest possible with respect to stability.<sup>10,12</sup> The temperatures obtained from the finite difference calculations for the examples 2 and 3 can be seen in Figs. 6 and 8 (marked as +). The maximum error is of

// This expression was chosen in order to use an existing program for an electronic calculator. A similar expression, but referring to the time  $t = (m + \frac{1}{2})\Delta t$  would be more consistent, but would not alter the order of magnitude of the truncation error given later.

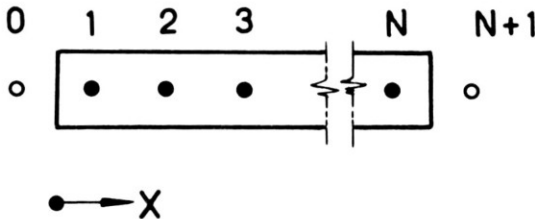


Fig. 9. Arrangement of auxiliary points 0 and  $N + 1$  in finite-difference calculations.

about the predicted size. Although these errors are acceptable for practical purposes, a deeper insight into the finite difference method is obtained as follows. Remember that the truncation error of Eq. (46) is higher than that of Eq. (44). Hence in order to improve the accuracy of solutions with a small number of sections in the skin, it would be more consistent to replace the boundary condition [Eq. (46)] by a corresponding expression with a smaller truncation error rather than to increase the number of sections. Besides, this way of improving accuracy is laborious, because a substantial increase in the accuracy could only be obtained by doubling the number of sections and then the computational work would increase by a factor 8, if maximum possible steps are used.<sup>12</sup> A finite difference approximation to Eq. (4) with a truncation error of

$$O \left[ (\Delta x)^4 \left( \frac{\partial^5 T}{\partial x^5} \right)_{N+1/2, m} \right]$$

is as follows:

$$\begin{aligned}
 T_{N+1, m+1} = & \frac{1}{105(1 + p_f) + 88p_r} \left\{ [105(1 - p_f) - 88p_r]T_{N+1, m} \right. \\
 + & [420(1 - p_f) + 68p_r]T_{N, m} + [-210(1 - p_f) + 36p_r]T_{N-1, m} \\
 + & [84(1 - p_f) - 20p_r]T_{N-2, m} + [-15(1 - p_f) + 4p_r]T_{N-3, m} \\
 + & [-420(1 + p_f) + 68p_r]T_{N, m+1} + [210(1 + p_f) + 36p_r] \\
 & T_{N-1, m+1} + [-84(1 + p_f) - 20p_r]T_{N-2, m+1} + \\
 & [15(1 + p_f) + 4p_r]T_{N-3, m+1} + 384p_r(T_{f, m} + T_{f, m+1}) \left. \right\} \quad (48) \\
 & + O \left[ (\Delta x)^4 \left( \frac{\partial^5 T}{\partial x^5} \right)_{N+1/2, m} \right]
 \end{aligned}$$

When Eq. (48) was used instead of Eq. (46) the results indicated in Figs. 6 and 8 by filled circles were obtained. The difference from the exact solutions is now only about 0.2 percent and the increase in computational work was about 20 percent. To obtain these results with Eq. (46) by increasing the number of sections would involve more than 6 times as much computational work.

Finally, an example is given which could not be solved by standard analytical methods. Consider example 3 (Fig. 7), with allowance now being made for a variation of  $h$ . A typical variation of  $h$  would be  $\pm 25$  percent of  $\bar{h}$  for an increase in  $T_f - T_i$  by an amount of  $500^\circ\text{C}$ , where  $\bar{h}$  is a mean value.  $h$  is assumed to increase linearly between  $0.75h$  to  $1.25h$  within 4 seconds and thereafter to fall by  $0.025h$  per sec. The variation of  $T_f$  and  $h$  are the same as previously for example 3, Fig. 7. For the sake of simplicity the finite difference method in its less complex form is used, with  $T_{N+1, m+1}$  being calculated according to Eq. (46). The skin is again divided into 5 sections. The distribution of temperature and stresses are shown in Fig. 10. Buckling occurs now after 6.53 sec as compared with a time of 7.45 sec for example 3, where a constant value  $h = \bar{h} = 0.07 \text{ kcal/m}^2 \text{ sec } ^\circ\text{C}$  was used.

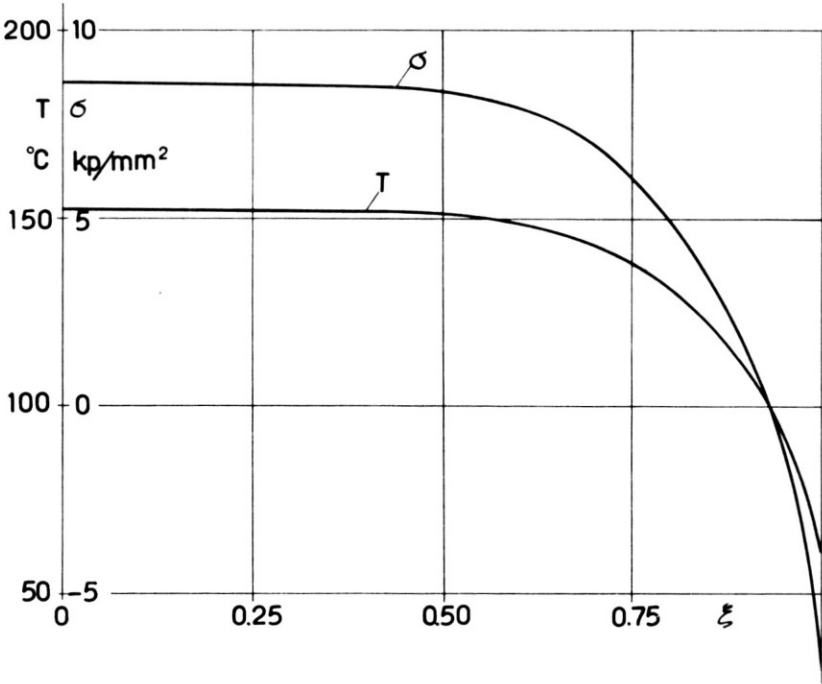


Fig. 10. As in Fig. 8, but variation of  $h$  taken into account.

### SUMMARY

A skin and a reinforcing frame are on their outer surfaces exposed to aerodynamic heating; the temperatures across the thickness of the skin and throughout the whole frame are assumed constant. An exact solution of the temperature distribution has been obtained by analytical methods and it is applicable for cases in which at least one of the two parameters of heat transfer, the heat transfer coefficient, is assumed to be constant. Because of this and other limitations of the analytical method, finite difference methods were also used and found to give excellent results for typical examples, even if the skin was, for the purpose of the difference calculations, divided into only five sections. The accuracy of the finite difference method used was still further improved by using higher order approximations in the boundary conditions. The stresses and buckling conditions within the elastic range were calculated by well-known methods.

### REFERENCES

1. Hoff, N. J., "Structural Problems of Future Aircraft," Third Anglo-American Aeronautical Conference at Brighton, England, 1951, Royal Aeronautical Society, pp. 77-114.
2. Parkes, E. W., "Transient Thermal Stresses in Wings," *Aircraft Engineering*, XXV, 1953, pp. 373-378.
3. Pohle, F. V., and H. Oliver, "Temperature Distribution and Thermal Stresses in a Model of a Supersonic Wing," *Jour. Aeron. Sci.*, vol. 21, no. 1, 1954, pp. 8-16.



4. Schuh, H., "Transient Temperature Distributions and Thermal Stresses in a Skin-shear Web Configuration at High-speed Flight for a Wide Range of Parameters," *Jour. Aeron. Sci.*, vol. 22, no. 2, 1955, pp. 829-837.
5. ———, "Heat Transfer in Structures," unpublished.
6. Carslaw, H. S., and J. C. Jaeger, "Conduction of Heat in Solids," *Sec. Ed.*, Oxford, 1959.
7. Timoshenko, S., *Theory of Elastic Stability*, New York, McGraw-Hill, 1936.
8. Schnell, W., and G. Fischer, "Berechnung der Beulwerte von Platten unter ungleichmässiger Temperaturbeanspruchung nach dem Mehrstellenverfahren," *DVL-Bericht*, No. 78, 1958.
9. Sommer, C. S., and B. I. Short, "Free-flight Measurements of Turbulent Boundary-layer Skin Friction in the Presence of Severe Aerodynamic Heating at Mach Numbers from 2.8 to 7.0," *NACA TN 3391*, 1955.
10. Richtmyer, R. D., *Difference Methods for Initial-value Problems*, New York, 1957.
11. Forsythe, G. E., and W. R. Wasow, *Finite Difference Methods for Partial Differential Equations*, New York, 1960.
12. Schuh, H., "Differenzenverfahren zum Berechnen von Temperatureausgleichsvorgängen bei eindimensionaler Wärmeströmung in einfachen und zusammengesetzten Körpern," *VDI-Forschungsheft*, 459, 1957.

*Discussor:* H. de l'Estoile, Direction des Recherches et Moyens D'Essais

Je voudrais simplement l'intérêt de la méthode des différences finies, qui est la seule utilisable quand la structure présente des discontinuités, par exemple des joints rivés ou collés.

A ce sujet, je suis heureux de constater que le Dr. Schuh vient de montrer que la méthode des différences finies est en excellent accord avec la méthode analytique.

*Author's reply to discussion:*

The finite difference method for calculating temperatures was extended in Ref. 12 of this paper, so that even cases with discontinuities in the structure, such as glued and riveted joints, can be treated.

